A Robust Proton Flux (pHlux) Assay for Studying the Function and Inhibition of the Influenza A M2 Proton Channel

Paul Santner,[†] João Miguel da Silva Martins,[†] Jonas S. Laursen,[‡] Lars Behrendt,[†] Leise Riber,[§] Christian A. Olsen,[‡,∥] Isaiah T. Arkin,[⊥] Jakob R. Winther,[†] Martin Willemoës,*,[†] and Kresten Lindorff-Larsen*,[†]

[†]Department of Biology, Section for Biomolecular Sciences, Linderstrøm-Lang Centre for Protein Science, University of Copenhagen, Ole Maaloes Vej 5, 2200 Copenhagen N, Denmark

[‡]Department of Drug Design and Pharmacology, Faculty of Health and Medical Sciences, University of Copenhagen, Universitetsparken 2, 2100 Copenhagen, Denmark

[§]Department of Biology, Section for Microbiology, University of Copenhagen, Ole Maaloes Vej 5, 2200 Copenhagen N, Denmark

[∥]Center for Biopharmaceuticals, Faculty of Health and Medical Sciences, University of Copenhagen, Universitetsparken 2, 2100 Copenhagen, Denmark

[⊥]Department of Biological Chemistry, The Hebrew University of Jerusalem, Edmond J. Safra Campus, Givat-Ram, Jerusalem 91904, Israel

ABSTRACT: The M2 protein is an important target for drugs in the fight against the influenza virus. Because of the emergence of resistance against antivirals directed toward the M2 proton channel, the search for new drugs against resistant M2 variants is of high importance. Robust and sensitive assays for testing potential drug compounds on different M2 variants are valuable tools in this search for new inhibitors. In this work, we describe a fluorescence sensor-based assay, which we termed "pHlux", that measures proton conduction through M2 when synthesized from an expression vector in *Escherichia coli*. The assay was compared to a previously established bacterial potassium ion transport complementation assay, and the results were compared to

simulations obtained from analysis of a computational model of M2 and its interaction with inhibitor molecules. The inhibition of M2 was measured for five different inhibitors, including Rimantadine, Amantadine, and spiro type compounds, and the drug resistance of the M2 mutant variants (swine flu, V27A, and S31N) was confirmed. We demonstrate that the pHlux assay is robust and highly sensitive and shows potential for high-throughput screening.
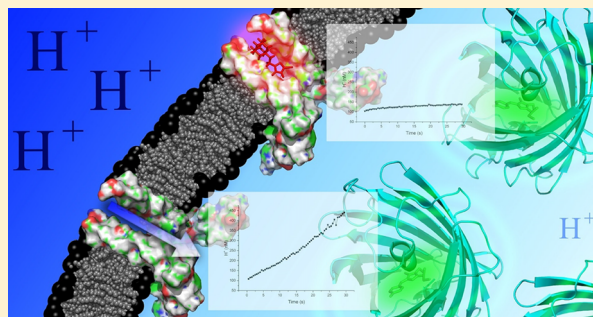
Influenza outbreaks annually cause 3−5 million cases of severe illness and 250000−500000 deaths.[1] Many different strategies for fighting influenza have been employed but are often hampered by the high adaptability of the virus.[2] The virus is known to readily cross the interspecies barrier via reassortment of its segmented genome and thus render a seasonal vaccination nearly ineffective.[3] To supplement these shortcomings of influenza vaccines, numerous antiviral compounds have been developed to target and inhibit crucial components of the infectious pathway of the virus.[4−6] The influenza A M2 proton channel is one of those targets, and the high mutation rate of the influenza virus has led to almost complete resistance against all known M2 inhibitors within four decades of their use.[7,8] M2 plays a crucial role in the infection of the host cell during the viral infectivity cycle.[9] Therefore, effective approaches for studying both potential M2 inhibitors and the development of resistance toward inhibitors are obviously of great importance.[10−16]

Previously published assays and screening procedures of M2 proton transport are typically low throughput and in addition require an elaborate experimental setup. Available experimental techniques include mammalian cell-based cytotoxicity or plaque reduction assays,[17,18] electrophysiological studies,[19] fusing a pH reporter protein, pHluorin, to M2,[20] and a liposome proton flux assay.[21] Other assays based on heterologous expression of M2 are the ion transport complementation of yeast[18] or bacteria[22] and growth inhibition by disruption of the proton motive force.[23] Methods that directly probe inhibitor binding include a tryptophan fluorescence-based approach[24] and isothermal titration calorimetry measurements.[25]

In this work, we describe a novel, easy, fast, and robust assay that provides a measure of M2 channel activity and inhibition
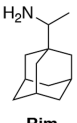
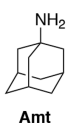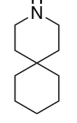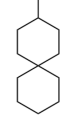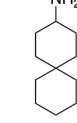and makes it feasible to screen a large number of compounds potentially targeting M2. The assay, termed "pHlux", is based on the expression of an inducible, codon-optimized M2 reading frame in an *Escherichia coli* strain that constitutively produces a ratiometric fluorescence pH sensor, pHluorin.[26,27] From cells harvested after induction of M2 expression and resuspended in buffer, the assay enables the quantification of M2-mediated changes in intracellular pH by conversion of the monitored fluorescence signal after a rapid lowering of the external pH. We have tested the pHlux assay on drug resistant and nonresistant M2 variants, analyzed their response to known inhibitors, and compared the results to those obtained using the M2 bacterial growth complementation assay.[22] In addition to the pHlux assay, we also report a computational model of M2 that aimed to predict implications for the structure of M2 upon inhibitor binding.[28,29]

■ EXPERIMENTAL PROCEDURES

Chemicals. Amantadine (Amt) and Rimantadine (Rim) were purchased from Sigma-Aldrich. 3-Aza-spiro[5.5]undecane (Azs) was purchased from Enamine. Spiro[5.5]undecan-3-ylmethanamine (Spm) and spiro[5.5]undecan-3-amine (Spa) were chemically synthesized from spiro[5.5]undecan-3-one, purchased from Atlantic SciTech Group, Inc., as previously described.[30] A structural overview of the inhibitors can be found in Table 1.

Table 1. Structural Overview of the M2 Inhibitors Used in This Study

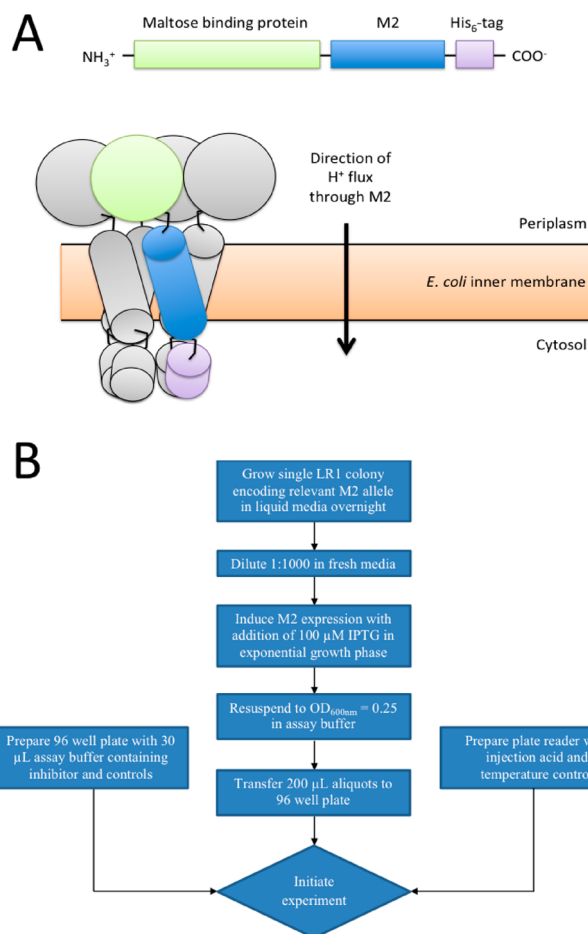| Rimantadine	Amantadine	3-Aza-spiro[5.5]undecane	Spiro[5.5]undecan-3-ylmethanamine	Spiro[5.5]undecan-3-amine
H_2N Rim	NH_2 Amt	H N Azs	NH_2 Spm	NH_2 Spa

Figure 1. Principles of the pHlux assay. (A) Schematic outline of the M2 proton channel transporter construct used in this work and its location in the *E. coli* inner membrane. The fusion protein incorporating the M2 channel (amino acid residues 1−97) is preceded by the maltose binding protein and followed by a six-residue His tag. Maltose binding protein facilitates the incorporation of the M2 transmembrane part into the inner membrane of *E. coli* to form the active tetramer conducting proton flux in the indicated direction. (B) Schematic outline of the procedure for the pHlux assay. The entire process is described in detail in Experimental Procedures.

Plasmids, Bacterial Strains, and Growth Media. All molecular biology was performed by conventional methods unless otherwise described. Nonresistant wild type M2 protein represented by the primary structure of the influenza A isolate Singapore/1/1957(H2N2)[31] and the M2 variant swine/Hong Kong/2011(H3N2), termed swine flu,[23] were produced from pMAL-p2X constructs, where the M2 reading frame is inserted in frame between those encoding an N-terminal maltose binding protein and a C-terminal His tag fusion (Figure 1A).[23] The point mutations that lead to the V27A and S31N side chain substitutions were introduced using the Quickchange mutagenesis method (Stratagene), according to the manufacturer's instructions.

The reading frame for the pH sensitive green fluorescent protein (pHluorin)[26] was amplified from plasmid pGFPR01,[27] using oligo-deoxyribonucleotides phluorin-fw-SD-EcoRI (CCCCC*GAATTC*ATGGAGATTAACTCAATCT<u>AGA-GGG</u>TATTAATAATGAGTAAAGGAGAAGAACTTTTCA-CTGGAGTTG) and phluorin-bw-wt-HindIII (CCCCC*AAG-CTTG*CTTTTATTTGTATAGTTCATCCATGCCATGTG-

TAATCCCAGCAGCTGTTAC) carrying a 5′ end overhang with the ribosome binding site of the murein-lipoprotein (Lpp) encoding gene of *E. coli* K-12,[32] as indicated by underlining and with restriction endonuclease sites for EcoRI and HindIII, respectively, shown in italics. The Lpp promoter was amplified directly from chromosomal DNA of *E. coli* K-12 MG1655[33] with oligo-deoxyribonucleotides Lpp-fw-SacI (CCCCC*GAGCTC*GATGAATCCGATGGAAGCATCC) and Lpp-bw-EcoRI (CCCCC*GAATTC*TAGCGTTACAAG-TATTACACAAAG) harboring the restriction sites for SacI and EcoRI, respectively, as indicated by italics. The amplified pHluorin reading frame and the Lpp promoter region were digested with either EcoRI and HindIII or SacI and EcoRI, respectively, and ligated into high-copy number plasmid pUC18T-mini-Tn7-Km[34] digested with SacI and HindIII, to allow for Lpp promoter-controlled expression of pHluorin. The resulting plasmid was verified by enzyme restriction analysis and detection of phenotypical fluorescence expression with an Axioscope 2 plus microscope (Zeiss) after transformation into *E. coli* strain MG1655.[33]

The pUC18T-mini-Tn7-Km derivative carrying the Lpp promoter:pHluorin fusion product (described above) was used as a template with oligo-deoxyribonucleotides Km-phluorin-GRG36-fw (CCCCC*GCGGCCGC*GACGGTATCGATAAG-CTAGCTTAATTAGCTG) and Km-phluorin-GRG36-bw (CCCCC*CCTAGG*CTGCAAGGCCTTCGCGAGGTACCG-GGC) to generate a polymerase chain reaction (PCR) product encoding the kanamycin resistance gene and the Lpp promoter:pHluorin fusion cassette flanked by NotI and AvrII restriction sites, as indicated by italics. The purified PCR product was ligated into the pGRG36 vector,[35] digested with both NotI and AvrII. The resulting plasmid was used to integrate the Lpp promoter:pHluorin fusion cassette together with the kanamycin resistance gene into the chromosomal lambda Tn7 attachment site of MG1655[33] by using a Tn7 transposon-based site specific integration approach as previously described.[35] The resulting strain, LR1, was verified by PCR demonstrating the chromosomal insertion, which was subsequently sequenced. Finally, pHluorin production was confirmed by flow cytometry with a FACSAria III system (BD Biosciences) and microscopy as described above.

LB650, a potassium uptake deficient *E. coli* strain[36] that can be complemented by expressing the M2 reading frame from pMAL-p2X,[23] was used for the growth assay as previously described.[22] Cells were grown in LB medium (10 g L^{-1} Tryptone, 5 g L^{-1} yeast extract, and 5 g L^{-1} NaCl, adjusted to pH 7.0 with NaOH pellets) and LBK medium (LB in which 100 μM KCl replaced NaCl). Ampicillin (100 μg mL^{-1}) and glucose (1%) were added to the medium, and cells were grown at 37 °C unless noted otherwise. For culture plates, the medium was solidified by addition of 1.5% agar. Liquid cultures of M2 and mutant variants, which were to be analyzed by the pHlux assay, were inoculated with single colonies isolated on culture plates.

Growth Assay. Growth of potassium uptake deficient *E. coli* strain LB650[36] is complemented by M2 expression as a surrogate for potassium transport.[22,37] LBK medium was used for growing cultures of LB650, transformed with pMal-p2x constructs harboring M2 or the relevant mutant variant. Cultures were grown overnight with vigorous agitation, the next day diluted in a 1:1000 ratio in fresh LBK medium, and grown for 3 h. Cells were subsequently harvested by centrifugation at 5000g for 5 min. The cell pellet was resuspended in LB medium to an OD$_{600}$ of 0.15, and 100 μL of the cell suspension was transferred to each well of a sterile 96-well plate (U-bottom 96 Well Polysterene, Greiner Bio-One). One volume of a mix of LB medium, IPTG, and M2 channel inhibitor was added to give a final IPTG concentration of 15 μM and inhibitor concentrations as stated in Results and Discussion. The 96-well plates also included controls (no inhibitor) and a blank (no cells). The 96-well plate was incubated in a microplate reader (Infinite M200 Pro, Tecan) at 25 °C with 30 × 15 min cycles of shaking at 300 rpm and 6 mm amplitude. Growth was monitored by OD$_{600}$ measurements (five flashes per read).

pHlux Assay. The workflow in the pHlux assay is schematically outlined in Figure 1B. First, synthesis of M2 and mutant variants was induced in exponential cultures of strain LR1, transformed with the relevant plasmids at an OD$_{600}$ of 0.5, by addition of 100 μM IPTG, and growth continued for 1 h. The cells were subsequently harvested as described above, resuspended, and diluted, to an OD$_{600}$ of 0.25, in assay buffer (McIlvaine buffer,[38] consisting of 200 mM Na$_2$HPO$_4$ and 0.9%

NaCl adjusted to pH 7.6 with 0.1 M citric acid). Aliquots of 200 μL of the cell suspension were transferred to a 96-well plate (Nunclon F96 MicroWell Black Polysterene, Thermo Fisher Scientific), each well already containing 30 μL of assay buffer with a range of drug concentrations as stated in Results and Discussion. A control (no inhibitor) and a blank (assay buffer only) were also included. The fluorescence measurements were taken at ambient temperature in a microplate reader (Infinite F200 Pro, Tecan) with two pairs of bandpass filters: two 520 nm emission filters [36 nm full width at half-maximum (fwhm), Edmund Optics] combined with 390 and 466 nm (40 nm fwhm, Edmund Optics) excitation filters. The fluorescence emissions of each well were measured by an alternating readout of the two filter pairs (one flash per read) for 60 cycles right after lowering the pH by addition of 70 μL of 300 mM citric acid and 0.9% NaCl (pH 2.0) using the liquid handling system of the instrument. The ratio of the two differently excited emissions [I_{390}/I_{466} (Figure 2A)] was calculated and translated into proton concentration [H$^+$] (in micromolar) from the interpolation described by eq 1 derived from the fluorescence ratio−proton concentration relationship shown in Figure 2B.

$$[\text{H}^+] = 0.132 \ \mu\text{M} \times \left(\frac{I_{390}}{I_{466}}\right)^{-1.75\left(\frac{I_{390}}{I_{466}}\right)^{-0.51}} \tag{1}$$

Proton fluxes (Figure 3) were calculated from the slope of a fit to the recorded data over a minimum time span of 5 s, starting at the earliest 5 s after addition of the titrant, to ensure reproducibility and complete equilibration after mixing.

Experiments were designed so that data measurements were limited to one 96-well plate at a time, with a total experimental run time of <1 h. The resulting data from proton flux measurements, Pflux, in the absence or presence of varying concentrations of the inhibitor, I, were fitted to eq 2, describing a standard binding isotherm with a basal (residual) proton flux, using nonlinear curve fitting in the OriginPro 9 software (OriginLab Corp.). The resulting parameters from the fitting are Pflux$_0$, the proton flux in the absence of the inhibitor, K_I, the inhibition constant for the inhibitor affecting M2 activity, and Pflux$_\text{res}$, the residual proton flux at an infinite inhibitor concentration.

$$P\text{flux} = \frac{P\text{flux}_0}{1 + \frac{[\text{I}]}{K_\text{I}}} + P\text{flux}_\text{res} \tag{2}$$

Growth rates, μ, obtained from growth curves in the presence of different concentrations of I, and μ_0, determined in the absence of the inhibitor, were fitted to eq 3 as described above for eq 2 to obtain the inhibitor constant, K_I.[22]

$$\mu = \frac{\mu_0}{1 + \frac{[\text{I}]}{K_\text{I}}} \tag{3}$$

Alchemical ΔG Calculations. All calculations were performed using Gromacs 5.0.6.[39] The CHARMM27 force field including the CMAP correction was used for the protein and water, with CHARMM36 force field parameters used for membrane lipids. The ligands' pK_a values were estimated with ChemAxon's pK_a predictor, and the major microspecies at pH 7 were parametrized using CGenFF.[40] A simulation system was built by expanding the protein structure (Protein Data Bank entry 2L0J), altered to the same sequence as the experimental
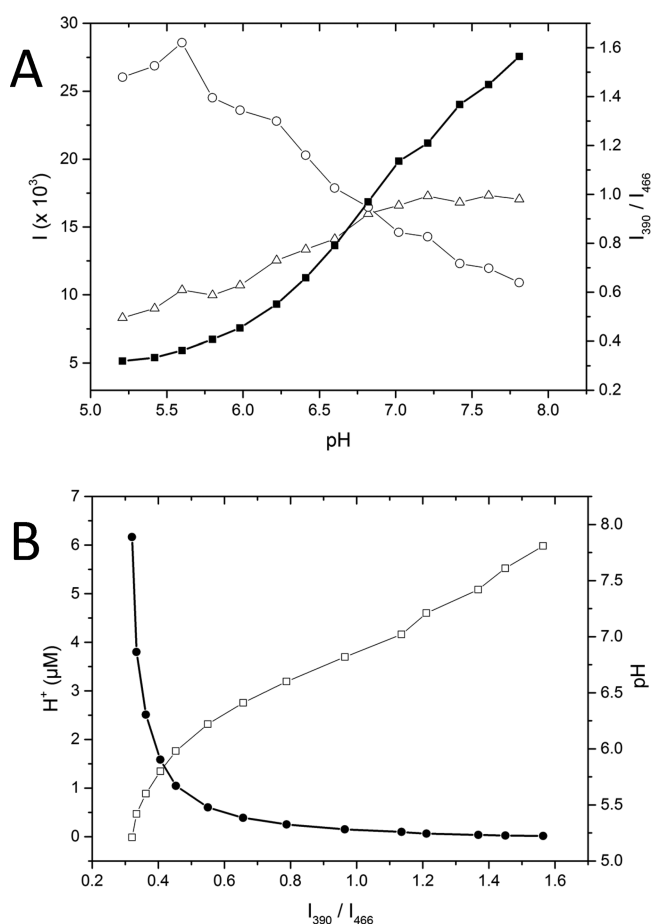
Figure 2. Relationship among fluorescence intensities, fluorescence intensity ratios, pH values, and proton concentrations for the pHlux assay. Experiments were performed as described in Experimental Procedures. (A) LR1 bacterial cells, containing overexpressed M2 protein, prepared under proton flux assay conditions were resuspended to an OD_{600} of 0.167 (accounting for missing dilution steps compared to the standard protocol) in assay buffers ranging from pH 5.2 to 7.8 in pH 0.2 steps. The intracellular and extracellular pH values were equilibrated until the fluorescence emission intensity ratios (I_{390}/I_{466}) remained constant ($\pm 1\%$ standard deviation). The emission intensities (I) were measured at 520 nm from excitations at ($\triangle$) 390 and ($\bigcirc$) 466 nm, and ($\blacksquare$) the I_{390}/I_{466} ratio was calculated. (B) Fluorescence emission intensity ratios from the standard curve at 390 and 466 nm (I_{390}/I_{466}) plotted vs ($\square$) pH values and ($\bullet$) proton concentrations. The black line represents the fit to eq 1 ($R^2 = 0.998$).

setting, inserted in a pre-equilibrated membrane using the inflateGRO script. The final system has 91892 atoms, 243 palmitoyloleoylphosphatidylethanolamine molecules, 19515 waters, 72 sodium cations, and 90 chloride anions. The M2 binding inhibitors were then manually placed inside the channel, in a position intersecting the plane formed by the four serine residues in position 31 and with the protonated amine pointing toward the histidine residues in position 37; the inhibitors were allowed to equilibrate for 50 ns, with the starting structure of the ALCHEMISTRY calculation being the last frame of this equilibration. All simulations were run in the semi-isotropic NPT ensemble at 1 bar and 310 K using 0.5 and 5 ps coupling constants for the barostat and thermostat, respectively. A single iteration of LINCS constraints (order of 4) was used to control the bonds involving hydrogen atoms, with a 2 fs integration time step by a stochastic dynamics

integrator. Both Coulombic and van der Waals interactions were calculated using particle mesh Ewald decomposition with a mesh spacing of 0.12 nm and an order of 4.

We used the double-decoupling method[28] with the virtual bond algorithm[29] to calculate ΔG. Ligand decoupling inside the pocket was divided in 33 λ intervals, the first 11 turning on the restrains relative to the protein, the next seven turning off Coulomb interactions between the ligand and the rest of the system, and the remaining 15 steps turning off the intermolecular van der Waals interactions of the ligand inside the pocket. The same intervals were used in the decoupling of the ligand in water. The restraining potentials that were used were kept for all protein−ligand state calculations and replicas, in accordance with the double-decoupling method, with increasing harmonic potential restraints scaled to 4184 kJ mol^{-1} nm^{-2}, 41.84 kJ mol^{-1} rad^{-2}, and 41.84 kJ mol^{-1} rad^{-2} for distances, angles, and dihedrals, respectively.

■ RESULTS AND DISCUSSION

We present here a novel and high-throughput ready system that couples M2-induced proton conduction in real time to a fluorescence output in the cytosol of *E. coli* cells (Figure 1). To facilitate the analysis of proton transport, we produced a standard curve (Figure 2A) described by eq 1 to derive the intracellular proton concentration based on the observed fluorescence signal (Figure 2B).

The versatility of the pHlux assay is clearly demonstrated in the analysis of the effect of known inhibitors, Rim and Amt, and the newly reported drug leads, Azs, Spm, and Spa,[30] on wild type and swine flu M2 protein. In addition, we analyzed two well-known single-amino acid changes leading to resistance in the wild type M2 background: S31N and V27A. For example, the assay clearly shows a substantial proton flux through wild type M2 channels at a level much greater than the very small background flux in cells that do not express M2 (Figure 3A). Furthermore, upon addition of Rim to the channels there is a substantial drop in flux, reaching background levels when the channels are saturated (Figure 3A). Similarly, the assay shows proton flux through the S31N (Figure 3B) and V27A (Figure 3C) channels and also reveals that this flux is not substantially decreased even in the presence of high concentrations of Rim, in line with the notion that these mutations give rise to drug resistant M2. To compare the performance of the pHlux assay, we also analyzed M2 inhibition using the previously published growth complementation assay[41] (Figure 4). K_I values of the various inhibitors calculated using data obtained from the growth assay or the proton flux are listed in Table 2. As expected for both assays, the drug resistant M2 variants were generally unaffected by inhibitor concentrations of ≤ 30 μM (data not shown).

Fluctuations in proton fluxes for similar incubations recorded in different wells within the same sample plate led us to conduct experiments with replica incubations distributed over the entire sample plate, but with no significant difference in the calculated values of K_I or Pflux$_{res}$ (data not shown).

Inhibition of M2 by Amt and Rim was demonstrated with both the growth assay and the pHlux assay, but only the pHlux assay resolved a difference in the affinity of M2 for the two inhibitors, as shown by the calculated K_I for the two compounds (Table 2). Furthermore, only with the pHlux assay did we detect inhibition by the spiro-molecule type compounds: Azs, Spm, and Spa. Curiously, Spa exerted stronger inhibition of wild type M2 than Amt, though both
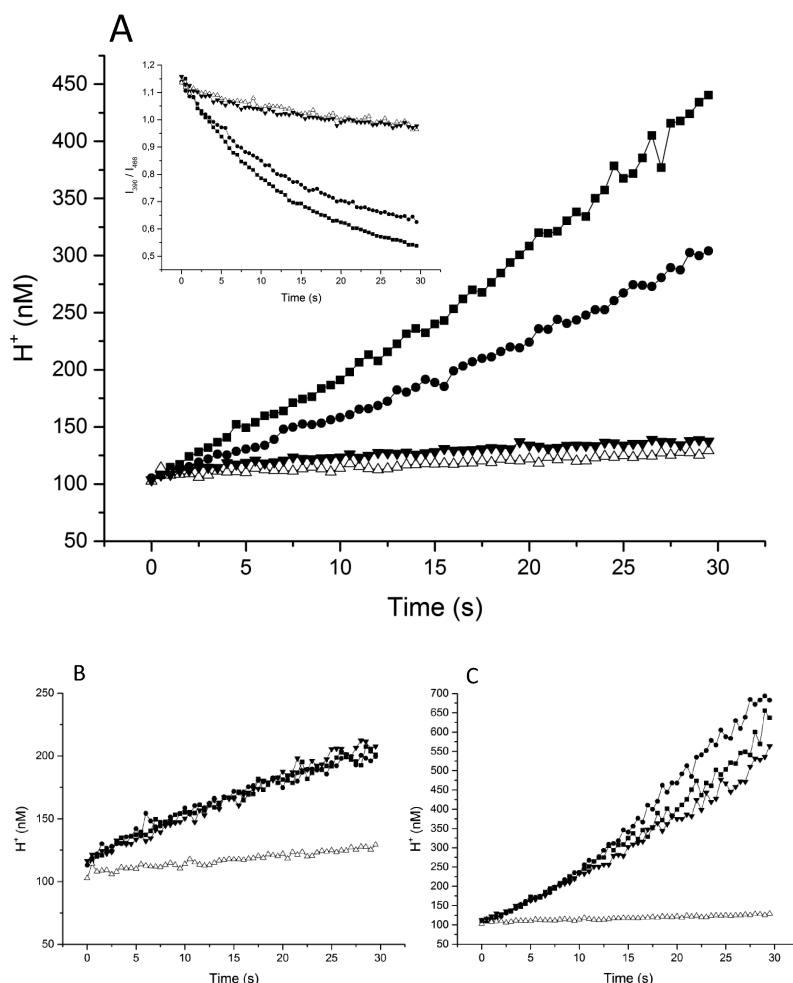
Figure 3. Rim inhibition of wild type, S31N, and V27A M2 proton channels. Experiments were performed as described in Experimental Procedures. Each line corresponds to individual wells of a 96-well plate containing an LR1 culture harboring M2 protein incubated at different inhibitor concentrations [(■) no inhibitor, (●) K_I, and (▼) $20K_I$, where K_I = 5.5 nM for binding of Rim to wild type M2] and a control [(△) no M2]. (A) Wild type M2. The inset shows the fluorescence intensity ratio determined from values measured at 390 and 466 nm (I_{390}/I_{466}) converted to give the proton concentrations in the main figure using eq 1. Similar experiments were performed for (B) S31N and (C) V27A, showing essentially no inhibition when Rim was added at the same concentrations used for wild type M2.
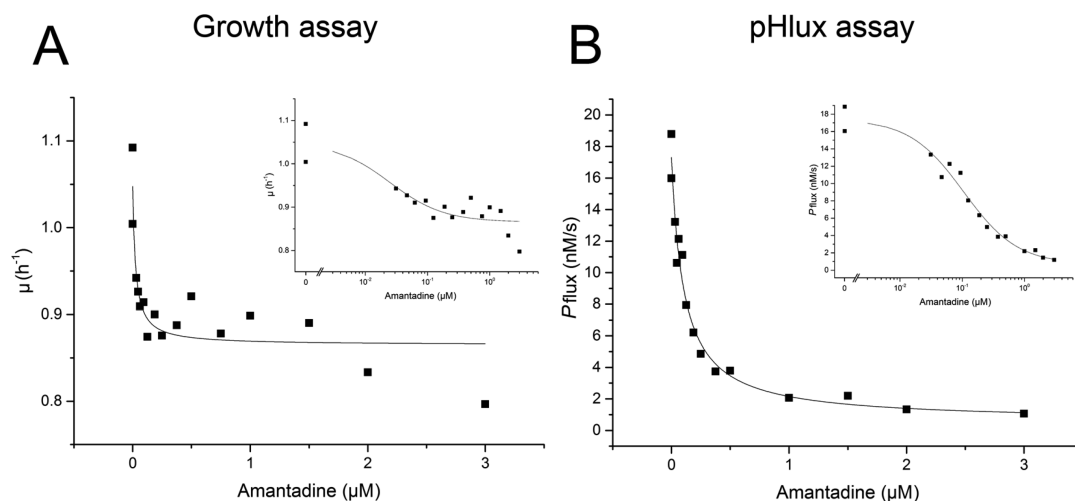

Figure 4. Comparison of the bacterial growth assay and the pHlux assay. Experiments were performed as described in Experimental Procedures. The inhibition of M2 by Amt was assessed using each assay. (A) Growth rates, μ, from the growth assay with the wild type M2 construct are plotted vs inhibitor concentration in the cell culture incubation and fitted to eq 3. (B) Pflux recorded using strain LR1 expressing the wild type M2 construct in the pHlux assay in the presence of an inhibitor and fitted to eq 2. The insets are log scale presentations of the same data.

Table 2. Parameters Determined for the Inhibition of Wild Type Influenza M2 Using Two Different Assays[a]

	pHlux assay[b]				growth assay[c]	
inhibitor	K_I (nM)	$P\text{flux}_{res}$ (nM s^{-1})	$P\text{flux}_0$ (nM s^{-1})	n[d]	K_I	n[d]
Rim	5.5 ± 0.4	0.4 ± 0.1	11.1 ± 0.2	5	21 ± 7 nM	3
Amt	63 ± 9	1 ± 0.3	12.8 ± 0.5	4	22 ± 9 nM	3
Azs	189 ± 18	0.23 ± 0.04	13.9 ± 0.3	4	>300 μM	3
Spm	304 ± 44	2.5 ± 0.2	13.8 ± 0.5	4	>300 μM	3
Spa	47 ± 5	1.2 ± 0.2	11.8 ± 0.3	4	>300 μM	3

[a]Experiments were performed as described in Experimental Procedures. [b]Parameters were obtained from fitting data from the pHlux assay to eq 2. [c]Parameters were obtained from fitting data from the growth assay to eq 3. [d]The number of independent experiments.

with similar $P\text{flux}_{res}$ values at full inhibitor saturation. None of the spiro type compounds inhibited V27A[30,42] when tested in the pHlux and growth assays, a result likely to be the cause of weaker inhibition and the inability to obtain sufficiently high inhibitor concentrations in the growth medium. Furthermore, inhibition of drug resistant variants of M2 with Amt and Rim, as reported previously in electrophysiological studies,[43,44] could not be confirmed with the pHlux assay. However, values of K_I for M2 inhibition obtained on the basis of the growth complementation assay employed here[22] and reported values determined by growth inhibition,[23] M2 tryptophan fluorescence,[24] and isothermal titration calorimetry[45] are all in good agreement with values of the pHlux assay listed in Table 2.

To supplement the experimental studies, we also performed computational studies of M2 and used a free energy perturbation method to calculate the free energy of binding (ΔG) for the interaction between M2 and the different small-molecule inhibitors. We also constructed structural models of the wild type and the two M2 variants, V27A and swine flu, to examine whether the computational model would be able to reproduce the resistance of these channels to the inhibitors. The results of the free energy calculations are listed in Table 3.

Table 3. Experimentally Derived and Computationally Calculated Binding Energies for Wild Type M2 Compared to Calculated Binding Energies for Drug Resistant M2 Variants

	calculated from measurements[a] (kcal mol^{-1})	computationally determined[b] (kcal mol^{-1})		
inhibitor	$\Delta G_{bind,WT}$	$\Delta G_{bind,WT}$	$\Delta G_{bind,V27A}$	$\Delta G_{bind,swine\ flu}$
Rim	−11.26 ± 0.04	−19 ± 7	13 ± 7	25 ± 7
Amt	−9.82 ± 0.09	−27 ± 3	2 ± 3	18 ± 3
Azs	−9.17 ± 0.06	−25 ± 1	1 ± 1	13 ± 1
Spm	−8.89 ± 0.09	−25 ± 5	3 ± 5	16 ± 5
Spa	−9.99 ± 0.07	−28 ± 4	0 ± 4	17 ± 4

[a]Calculated from $\Delta G_{bind,WT} = RT \ln(K_I \times 1\ M^{-1})$ using values of K_I in molar obtained from the pHlux assay listed in Table 2 obtained at 25 °C as described in Experimental Procedures. [b]ALCHEMISTRY calculations were performed as described in Experimental Procedures.

We observe a dramatic decrease in affinity between the inhibitors and M2 in the resistance mutants (~30 and ~40 kcal mol^{-1} for V27A and the swine flu variant, respectively). Thus, the result from analysis of the computational models of wild type and mutant M2 indicates that structural determinants for the resistance of mutant M2 variants may be predicted from the computational models and that the models can aid in interpreting experimental data.

Second, we find that the computations cannot rank the affinity of the different inhibitors for wild type M2 and that instead the affinities of all five ligands are within error of one another. Thus, with the computational approach and resources used here, our free energy calculations are more useful for detecting the large drop in affinity that results from accumulation of the resistance mutation than for selecting individual inhibitors.

The origin of the residual flux component, $P\text{flux}_{res}$, in eq 2 is still unclear. One interpretation could be that it represents proton leakage through M2 even with a bound inhibitor. We find, however, that cells overproducing only the maltose binding protein from the pMAL-p2X vector lead to observed proton fluxes of ~1.2 nM s^{-1}, which is higher than, e.g., the $P\text{flux}_{res}$ of M2 inhibited by Rim. Nevertheless, we suggest that $P\text{flux}_{res}$ can be a useful parameter in evaluating inhibitor properties in more detail, as an increased $P\text{flux}_{res}$ displayed by M2 variants with a bound inhibitor may still allow that given M2 variant to promote virus infectivity.[19,46−48]

Even though the spiro-based inhibitors failed to inhibit resistant M2 mutant proteins when tested in the pHlux assay, they were able to inhibit the wild type M2 channel. The divergent chemical structures of these candidate inhibitors compared to those of Amt and Rim suggest that an alternative molecular architecture may form the basis for new generations of M2 inhibitors[49] as it is already being exploited in drug design.[12,30,42,43,50,51]

■ CONCLUSIONS

We have developed and validated a novel, quantitative assay for measuring proton conduction through the M2 proton channel, by expressing the channel in a bacterial strain that also expresses the pH-dependent fluorescent protein, pHluorin. Upon a jump in extracellular proton concentration, it is thus possible to use a fluorescence-enabled plate reader to measure M2-mediated proton flux across the bacterial membrane. The ability to measure M2 activity easily and rapidly and in a high-throughput manner in turn enabled us to use the assay to determine the inhibition constants for a series of small molecules that are known to bind to M2. Given the ease of use and quantitative results, we expect that the pHlux assay, potentially in combination with computational structural models of M2 and variants, will prove to be a valuable tool in elucidating the structure−function relations in M2 as already demonstrated in ref 52.

■ AUTHOR INFORMATION

Corresponding Authors
*E-mail: lindorff@bio.ku.dk.
*E-mail: willemoes@bio.ku.dk.

ORCID 🔵

Christian A. Olsen: 0000-0002-2953-8942
Jakob R. Winther: 0000-0001-6995-9154
Martin Willemoës: 0000-0003-1689-2712
Kresten Lindorff-Larsen: 0000-0002-4750-6039

Notes

The authors declare no competing financial interest.

Mutant enzymes are abbreviated according to the position of the changed residue, e.g., S31N indicating a single-amino acid alteration at position 31 from serine to asparagine.

■ ABBREVIATIONS

Amt, Amantadine; Azs, 3-aza-spiro[5.5]undecane; IPTG, isopropyl β-D-thiogalactopyranoside; Rim, Rimantadine; Spa, spiro[5.5]undecan-3-amine; Spm, spiro[5.5]undecan-3-ylmethanamine.

■ REFERENCES

(1) World Health Organization (2014) Fact sheet N° 122 on influenza. http://www.who.int/mediacentre/factsheets/fs211/en/ (accessed March 14, 2016).

(2) Gottlieb, T., and Ben-Yedidia, T. (2014) Epitope-based approaches to a universal influenza vaccine. *J. Autoimmun. 54*, 15−20.

(3) Pebody, R., Warburton, F., Ellis, J., Andrews, N., Thompson, C., von Wissmann, B., Green, H., Cottrell, S., Johnston, J., de Lusignan, S., Moore, C., Gunson, R., Robertson, C., McMenamin, J., and Zambon, M. (2015) Low effectiveness of seasonal influenza vaccine in preventing laboratory-confirmed influenza in primary care in the United Kingdom: 2014/15 mid−season results. *Eurosurveillance 20*, 21025.

(4) Ludwig, S., Zell, R., Schwemmle, M., and Herold, S. (2014) Influenza, a One Health paradigm—Novel therapeutic strategies to fight a zoonotic pathogen with pandemic potential. *Int. J. Med. Microbiol. 304*, 894−901.

(5) Zarubaev, V. V., Garshinina, A. V., Tretiak, T. S., Fedorova, V. A., Shtro, A. A., Sokolova, A. S., Yarovaya, O. I., and Salakhutdinov, N. F. (2015) Broad range of inhibiting action of novel camphor-based compound with anti-hemagglutinin activity against influenza viruses in vitro and in vivo. *Antiviral Res. 120*, 126−133.

(6) Sutton, T. C., Obadan, A., Lavigne, J., Chen, H., Li, W., and Perez, D. R. (2014) Genome rearrangement of influenza virus for anti-viral drug screening. *Virus Res. 189*, 14−23.

(7) Nelson, M. I., Simonsen, L., Viboud, C., Miller, M. A., and Holmes, E. C. (2009) The origin and global emergence of adamantane resistant A/H3N2 influenza viruses. *Virology 388*, 270−278.

(8) Dong, G., Peng, C., Luo, J., Wang, C., Han, L., Wu, B., Ji, G., and He, H. (2015) Adamantane-Resistant Influenza A Viruses in the World (1902−2013): Frequency and Distribution of M2 Gene Mutations. *PLoS One 10*, e0119115.

(9) Pinto, L. H., Holsinger, L. J., and Lamb, R. A. (1992) Influenza virus M2 protein has ion channel activity. *Cell 69*, 517−528.

(10) El-Shesheny, R., Bagato, O., Kandeil, A., Mostafa, A., Mahmoud, S. H., Hassanneen, H. M., Webby, R. J., Ali, M. A., and Kayali, G. (2016) Re-emergence of amantadine-resistant variants among highly pathogenic avian influenza H5N1 viruses in Egypt. *Infect., Genet. Evol. 46*, 102−109.

(11) Hu, Y., Musharrafieh, R., Ma, C., Zhang, J., Smee, D. F., DeGrado, W. F., and Wang, J. (2017) An M2-V27A channel blocker demonstrates potent in vitro and in vivo antiviral activities against amantadine-sensitive and -resistant influenza A viruses. *Antiviral Res. 140*, 45−54.

(12) Li, F., Ma, C., DeGrado, W. F., and Wang, J. (2016) Discovery of Highly Potent Inhibitors Targeting the Predominant Drug-Resistant S31N Mutant of the Influenza A Virus M2 Proton Channel. *J. Med. Chem. 59*, 1207−1216.

(13) Ma, C., Zhang, J., and Wang, J. (2016) Pharmacological Characterization of the Spectrum of Antiviral Activity and Genetic Barrier to Drug Resistance of M2-S31N Channel Blockers. *Mol. Pharmacol. 90*, 188−198.

(14) Jalily, P. H., Eldstrom, J., Miller, S. C., Kwan, D. C., Tai, S. S.-H., Chou, D., Niikura, M., Tietjen, I., and Fedida, D. (2016) Mechanisms of action of novel influenza A/M2 viroporin inhibitors derived from hexamethylene amiloride. *Mol. Pharmacol. 90*, 80−95.

(15) Arns, S., Balgi, A. D., Shimizu, Y., Pfeifer, T. A., Kumar, N., Shidmoossavee, F. S., Sun, S., Tai, S. S.-H., Agafitei, O., Jaquith, J. B., Bourque, E., Niikura, M., and Roberge, M. (2016) Novel spirothiazamenthane inhibitors of the influenza A M2 proton channel. *Eur. J. Med. Chem. 120*, 64−73.

(16) Klimochkin, Y. N., Shiryaev, V. A., Petrov, P. V., Radchenko, E. V., Palyulin, V. A., and Zefirov, N. S. (2016) Design of Broad-Spectrum Inhibitors of Influenza A Virus M2 Proton Channels: A Molecular Modeling Approach. *Curr. Comput.-Aided Drug Des. 12*, 154−164.

(17) Si, Y., Li, J., Niu, Y., Liu, X., Ren, L., Guo, L., Cheng, M., Zhou, H., Wang, J., Jin, Q., and Yang, W. (2014) Entry Properties and Entry Inhibitors of a Human H7N9 Influenza Virus. *PLoS One 9*, e107235.

(18) Balgi, A. D., Wang, J., Cheng, D. Y. H., Ma, C., Pfeifer, T. A., Shimizu, Y., Anderson, H. J., Pinto, L. H., Lamb, R. A., DeGrado, W. F., and Roberge, M. (2013) Inhibitors of the Influenza A Virus M2 Proton Channel Discovered Using a High-Throughput Yeast Growth Restoration Assay. *PLoS One 8*, e55271.

(19) Balannik, V., Carnevale, V., Fiorin, G., Levine, B. G., Lamb, R. A., Klein, M. L., DeGrado, W. F., and Pinto, L. H. (2010) Functional Studies and Modeling of Pore-Lining Residue Mutants of the Influenza A Virus M2 Ion Channel. *Biochemistry 49*, 696−708.

(20) Balannik, V., Obrdlik, P., Inayat, S., Steensen, C., Wang, J., Rausch, J. M., DeGrado, W. F., Kelety, B., and Pinto, L. H. (2010) Solid-supported membrane technology for the investigation of the influenza A virus M2 channel activity. *Pfluegers Arch. 459*, 593−605.

(21) Pielak, R. M., Schnell, J. R., and Chou, J. J. (2009) Mechanism of drug inhibition and drug resistance of influenza A M2 channel. *Proc. Natl. Acad. Sci. U. S. A. 106*, 7379−7384.

(22) Assa, D., Alhadeff, R., Krugliak, M., and Arkin, I. T. (2016) Mapping the Resistance Potential of Influenza's H+ Channel against an Antiviral Blocker. *J. Mol. Biol. 428*, 4209−4217.

(23) Astrahan, P., Flitman-Tene, R., Bennett, E. R., Krugliak, M., Gilon, C., and Arkin, I. T. (2011) Quantitative analysis of influenza M2 channel blockers. *Biochim. Biophys. Acta, Biomembr. 1808*, 394−398.

(24) Eleftheratos, S., Spearpoint, P., Ortore, G., Kolocouris, A., Martinelli, A., Martin, S., and Hay, A. (2010) Interaction of aminoadamantane derivatives with the influenza A virus M2 channel-Docking using a pore blocking model. *Bioorg. Med. Chem. Lett. 20*, 4182−4187.

(25) Ioannidis, H., Drakopoulos, A., Tzitzoglaki, C., Homeyer, N., Kolarov, F., Gkeka, P., Freudenberger, K.-M., Liolios, C. C., Gauglitz, G., Cournia, Z., Gohlke, H., and Kolocouris, A. (2016) Alchemical Free Energy Calculations and Isothermal Titration Calorimetry Measurements of Aminoadamantanes Bound to the Closed State of Influenza A/M2TM. *J. Chem. Inf. Model. 56*, 862−76.

(26) Miesenböck, G., De Angelis, D. A., and Rothman, J. E. (1998) Visualizing secretion and synaptic transmission with pH-sensitive green fluorescent proteins. *Nature 394*, 192−195.

(27) Martinez, K. A., 2nd, Kitko, R. D., Mershon, J. P., Adcox, H. E., Malek, K. A., Berkmen, M. B., and Slonczewski, J. L. (2012) Cytoplasmic pH response to acid stress in individual cells of Escherichia coli and Bacillus subtilis observed by fluorescence ratio imaging microscopy. *Appl. Environ. Microbiol. 78*, 3706−3714.

(28) Gilson, M. K., Given, J. A., Bush, B. L., and McCammon, J. A. (1997) The statistical-thermodynamic basis for computation of binding affinities: a critical review. *Biophys. J. 72*, 1047−1069.

(29) Boresch, S., Tettinger, F., Leitgeb, M., and Karplus, M. (2003) Absolute Binding Free Energies: A Quantitative Approach for Their Calculation. *J. Phys. Chem. B 107*, 9535−9551.

(30) Wang, J., Ma, C., Fiorin, G., Carnevale, V., Wang, T., Hu, F., Lamb, R. A., Pinto, L. H., Hong, M., Klein, M. L., and DeGrado, W. F. (2011) Molecular Dynamics Simulation Directed Rational Design of Inhibitors Targeting Drug-Resistant Mutants of Influenza A Virus M2. *J. Am. Chem. Soc. 133*, 12834−12841.

(31) Hay, A. J., Wolstenholme, A. J., Skehel, J. J., and Smith, M. H. (1985) The molecular basis of the specific anti-influenza action of amantadine. *EMBO J. 4*, 3021−3024.

(32) Nakamura, K., and Inouye, M. (1979) DNA sequence of the gene for the outer membrane lipoprotein of E. coli: an extremely AT-rich promoter. *Cell 18*, 1109−1117.

(33) Blattner, F. R., Plunkett, G., Bloch, C. A., Perna, N. T., Burland, V., Riley, M., Collado-Vides, J., Glasner, J. D., Rode, C. K., Mayhew, G. F., Gregor, J., Davis, N. W., Kirkpatrick, H. A., Goeden, M. A., Rose, D. J., Mau, B., and Shao, Y. (1997) The Complete Genome Sequence of Escherichia coli K-12. *Science 277*, 1453−1462.

(34) Choi, K.-H., Gaynor, J. B., White, K. G., Lopez, C., Bosio, C. M., Karkhoff-Schweizer, R. R., and Schweizer, H. P. (2005) A Tn7-based broad-range bacterial cloning and expression system. *Nat. Methods 2*, 443−448.

(35) McKenzie, G. J., and Craig, N. L. (2006) Fast, easy and efficient: site-specific insertion of transgenes into Enterobacterial chromosomes using Tn7 without need for selection of the insertion event. *BMC Microbiol. 6*, 39.

(36) Stumpe, S., and Bakker, E. P. (1997) Requirement of a large K+-uptake capacity and of extracytoplasmic protease activity for protamine resistance of Escherichia coli. *Arch. Microbiol. 167*, 126−136.

(37) Leiding, T., Wang, J., Martinsson, J., DeGrado, W. F., and Årsköld, S. P. (2010) Proton and cation transport activity of the M2 proton channel from influenza A virus. *Proc. Natl. Acad. Sci. U. S. A. 107*, 15409−15414.

(38) McIlvaine, T. C. (1921) A Buffer Solution for Colorimetric Comparison. *J. Biol. Chem. 49*, 183−186.

(39) Abraham, M. J., Murtola, T., Schulz, R., Páll, S., Smith, J. C., Hess, B., and Lindahl, E. (2015) GROMACS: High performance molecular simulations through multi-level parallelism from laptops to supercomputers. *SoftwareX 1−2*, 19−25.

(40) Vanommeslaeghe, K., Hatcher, E., Acharya, C., Kundu, S., Zhong, S., Shim, J., Darian, E., Guvench, O., Lopes, P., Vorobyov, I., and Mackerell, A. D. (2010) CHARMM general force field: A force field for drug-like molecules compatible with the CHARMM all-atom additive biological force fields. *J. Comput. Chem. 31*, 671−690.

(41) Taube, R., Alhadeff, R., Assa, D., Krugliak, M., and Arkin, I. T. (2014) Bacteria-Based Analysis of HIV-1 Vpu Channel Activity. *PLoS One 9*, e105387.

(42) Balannik, V., Wang, J., Ohigashi, Y., Jing, X., Magavern, E., Lamb, R. A., DeGrado, W. F., and Pinto, L. H. (2009) Design and Pharmacological Characterization of Inhibitors of Amantadine-Resistant Mutants of the M2 Ion Channel of Influenza A Virus. *Biochemistry 48*, 11872−11882.

(43) Wang, J., Ma, C., Wang, J., Jo, H., Canturk, B., Fiorin, G., Pinto, L. H., Lamb, R. A., Klein, M. L., and DeGrado, W. F. (2013) Discovery of Novel Dual Inhibitors of the Wild-Type and the Most Prevalent Drug-Resistant Mutant, S31N, of the M2 Proton Channel from Influenza A Virus. *J. Med. Chem. 56*, 2804−2812.

(44) Kolocouris, A., Tzitzoglaki, C., Johnson, F. B., Zell, R., Wright, A. K., Cross, T. A., Tietjen, I., Fedida, D., and Busath, D. D. (2014) Aminoadamantanes with persistent in vitro efficacy against H1N1 (2009) influenza A. *J. Med. Chem. 57*, 4629−4639.

(45) Homeyer, N., Ioannidis, H., Kolarov, F., Gauglitz, G., Zikos, C., Kolocouris, A., and Gohlke, H. (2016) Interpreting Thermodynamic Profiles of Aminoadamantane Compounds Inhibiting the M2 Proton

Channel of Influenza A by Free Energy Calculations. *J. Chem. Inf. Model. 56*, 110−126.

(46) Grambas, S., and Hay, A. J. (1992) Maturation of influenza a virus hemagglutinin—Estimates of the pH encountered during transport and its regulation by the M2 protein. *Virology 190*, 11−18.

(47) Costello, D. A., Whittaker, G. R., and Daniel, S. (2015) Variations in pH Sensitivity, Acid Stability, and Fusogenicity of Three Influenza Virus H3 Subtypes. *J. Virol. 89*, 350−360.

(48) Leonov, H., Astrahan, P., Krugliak, M., and Arkin, I. T. (2011) How Do Aminoadamantanes Block the Influenza M2 Channel, and How Does Resistance Develop? *J. Am. Chem. Soc. 133*, 9903−9911.

(49) Alhadeff, R., Assa, D., Astrahan, P., Krugliak, M., and Arkin, I. T. (2014) Computational and experimental analysis of drug binding to the Influenza M2 channel. *Biochim. Biophys. Acta, Biomembr. 1838*, 1068−73.

(50) Du, Q. S., Huang, R. B., Wang, S. Q., and Chou, K. C. (2010) Designing Inhibitors of M2 Proton Channel against H1N1 Swine Influenza Virus. *PLoS One 5*, e9388.

(51) Wang, J., Li, F., and Ma, C. (2015) Recent progress in designing inhibitors that target the drug-resistant M2 proton channels from the influenza A viruses. *Biopolymers 104*, 291−309.

(52) Santner, P., Martins, J. M. d. S., Kampmeyer, C., Hartmann-Petersen, R., Laursen, J. S., Stein, A., Olsen, C. A., Arkin, I. T., Winther, J. R., Willemoës, M., and Lindorff-Larsen, K. (2018) Random mutagenesis analysis of the influenza A M2 proton channel reveals novel resistance mutants. *Biochemistry*, DOI: 10.1021/acs.biochem.8b00722.